RELACIÓN ESPECTRAL ENTRE LAS OLAS OCEÁNICAS Y EL RUIDO MICROSMÍSMICO: UN ANÁLISIS DIÁDICO UTILIZANDO EL TE-GRAM

Diego Seuret-Jiménez [(1)], Daily Quintana-Fuentes [(1,)], José Manuel Nieto-Jalil [(2)], Eduardo Trutié-Carrero [(1)] and J. Jesús Escobedo-Alatorre [(1)]*

RESUMEN

Comprender los mecanismos de acoplamiento entre la dinámica oceánica y el ruido sísmico ambiental sigue siendo un desafío fundamental en la ciencia. Este estudio introduce un análisis espectral de alta resolución entre señales sísmicas y ondas oceánicas utilizando el Te-gram, una herramienta matemática diseñada para superar las limitaciones de los métodos clásicos de tiempo-frecuencia. Se analizan dos eventos sísmicos cerca de Baja California, ocurridos el 22 de abril de 2021 y el 15 de septiembre de 2022, junto con datos del oleaje de la estación 155 del CDIP. Los resultados revelan picos de energía persistentes centrados en 0.07 Hz tanto en los registros marinos como en los sísmicos. Esta frecuencia coincide con la banda principal de microsismos y es indicativa de interacciones directas en el fondo marino impulsadas por el oleaje oceánico de período largo. El análisis comparativo con herramientas espectrales convencionales demuestra la capacidad superior del Te-gram. Los resultados obtenidos refuerzan la hipótesis de que el incremento de energía del oleaje en la banda microsísmica corresponde con el aumento de la energía sísmica en la misma frecuencia, lo que sugiere una transferencia continua de energía entre el océano y la Tierra sólida. Estos hallazgos contribuyen a la comprensión geofísica de cómo las condiciones oceanográficas persistentes pueden influir en las oscilaciones de fondo de la litosfera.

Palabras clave: Te-gram; ruido de la Tierra; microsismo primario; microsismo secundario

ISSN-e 2395-8251

SPECTRAL RELATIONSHIP BETWEEN OCEAN WAVES AND MICROSEISMIC NOISE: A DYADIC ANALYSIS USING TE-GRAM

ABSTRACT

Understanding the coupling mechanisms between ocean dynamics and ambient seismic noise remains a fundamental challenge in Earth system science. This study introduces a high-resolution spectral analysis between seismic signals and ocean waves using the Te-gram, a mathematical tool designed to overcome the limitations of classical time-frequency methods. Two local seismic events near Baja California, occurring on April 22, 2021 (Mw 3.8) and September 15, 2022 (Mw 4.1), were analyzed,

Artículo recibido el 31 de marzo de 2026 y aprobado para su publicación el 27 de octubre de 2026. Se aceptarán comentarios y/o discusiones hasta cinco meses después de su publicación.

[(1)] Centro de Investigación en Ingeniería y Ciencias Aplicadas, Universidad Autónoma del Estado de Morelos, Campus Chamilpa, Ave. Universidad 1001, Col. Chamilpa, Cuernavaca CP 62209, México; dseuret@uaem.mx (D.S.-J.); daily.quintana@uaem.edu.mx (D.Q.-F.); eduardo.trutie@uaem.edu.mx (E.T.-C.); jescobedo@uaem.mx (J.J.E.-A.).
* Correspondence: Daily Quintana Fuentes, daily.quintana@uaem.edu.mx (D.Q.-F.)

[(2)] Tecnológico de Monterrey, School of Engineering and Sciences, Atlixcayotl 5718, Reserva Territorial Atlixcayotl, CP 72453 Puebla, Puebla, México; jnietoj@tec.mx

along with wave acceleration data from CDIP station 155. The results reveal persistent energy peaks centered at 0.07 Hz in both marine and seismic records, consistently observed across multiple time windows. This frequency aligns with the primary microseism band and is indicative of direct seafloor interactions driven by long-period ocean swell. Comparative analysis with conventional spectral tools demonstrates the Te-gram superior ability to suppress cross-terms, resolve localized energy, and preserve nonstationary signal features. Control period comparisons further reinforce the hypothesis that enhanced wave energy in the microseismic band corresponds with increased seismic energy at the same frequency, suggesting continuous ocean–solid Earth energy transfer. These findings contribute to the geophysical understanding of how persistent oceanographic conditions can influence the lithosphere's background oscillations.

Keywords: Te-gram; Earth's noise; primary-microseism; secondary-microseism

INTRODUCTION

This paper presents a new approach to analyzing the relationship between background seismic noise and ocean wave frequencies, along with a new application of the mathematical tool Te-gram, first defined by Seuret-Jimenez et al. (2023). This approach refers to an empirical induction obtained from the analysis of measurements, applying the Te-gram to the vibrations produced by ocean waves hitting the coast and to the signals recorded as background seismic noise or Earth noise. To date, no study in the scientific literature has used this new approach to demonstrate the causal relationship between coastal wave buffeting and Earth noise.

ISSN-e 2395-8251

Seismic background noise, often perceived as a nuisance in classical seismological analysis, has gained increasing relevance as a signal source capable of revealing dynamic Earth processes. Commonly recorded by broadband seismic networks worldwide, this "ambient seismic noise" consists of continuous ground motion with diverse spectral content, providing valuable insights into both natural and anthropogenic phenomena. In recent years, researchers have leveraged background noise to monitor changes in the Earth's crust, image subsurface structures, and explore interactions between the solid Earth and the ocean-atmosphere system. Among the natural sources of seismic noise, ocean wave activity stands out as a major contributor, particularly in the generation of low-frequency microseisms that manifest in well-defined spectral bands (Schweitzer, 1911; Hinde and Gaunt, 1967; Asten, 1978; Bonnefoy-Claudet et al., 2006; Shubladze and Tsereteli, 2023).

Microseisms, typically detected within the 0.02–0.4 Hz range, are classified into two primary categories (Castrillo, 2013; Buffoni, 2016; Lunansky, 2019): primary microseisms, observed around 0.07–0.1 Hz, and secondary microseisms, located near 0.14–0.2 Hz (Friedrich et al., 1998; Schulte-Pelkum et al., 2004; Stutzmann et al., 2012). These oscillations are generated by the interaction of oceanic surface gravity waves with the seabed and through nonlinear interference between waves traveling in opposing directions. In shallow water, wave-seabed interaction leads to vertical pressure fluctuations that transfer energy into the solid Earth, producing primary microseisms (Hasselmann, 1963; Haubrich et al., 1963; Ardhuin et al., 2015). Conversely, secondary microseisms originate from the interaction of counter-propagating wave systems, such as oceanic waves generated by storms and those reflected off the coast, leading to a frequency-doubling phenomenon (Longuet-Higgins, 1950; Tanimoto, 2007; Ardhuin et al., 2011; Retailleau and Gualtieri, 2021).

The close relationship between wave energy and microseismic activity has been recognized since the mid-20th century, with notable studies confirming spatial and temporal correlations between ocean wave fields and seismic energy. Essen et al. (2003) demonstrated that microseisms in Norway and northern

Germany correlate strongly with swell activity off the southwest coast of Norway. Similarly, Tanimoto et al. (2006**)** and Schulte-Pelkum et al. (2004) applied polarization and coherence analysis to seismic arrays in the western United States, showing that ocean wave conditions modulate the energy and directional properties of ambient noise.

Stehly et al. (2006) proposed that primary microseisms exhibit seasonal variability very similar to the behavior of long-period noise. In this research, the authors used cross-correlations of continuous vertical records for each of the paths traced between pairs of stations in various networks on the east coast of the United States, Western Europe, and Tanzania. Webb (2007) presented a modified analysis of the original expression developed by Hasselmann (1963) on the generation of microseisms in seismically quiet zones. This study suggests that the Earth's "hum" at frequencies from 2 mHz to 40 mHz is driven by ocean waves over continental shelves; however, their model diverges for frequencies above 40 mHz.

Additional studies have validated these findings using frequency-domain and back-projection methods, linking specific storm events and tropical cyclones to microseismic excitation (Tanimoto, 2007**;** Nishida et al., 2008**;** Kedar et al., 2008**;** Traer and Gerstoft, 2014**;** Retailleau and Gualtieri, 2021).

Despite the increasing body of literature addressing the ocean-seismic coupling, a significant methodological gap persists. Most studies rely on Fourier-based methods or time-domain cross-correlations that assume stationarity or fail to isolate fine-grained energy structures in complex, stochastic signals. While the Fourier Transform provides the spectral content of a signal, it lacks temporal localization and is particularly unsuitable for the detection of evolving or intermittent features in background noise (Quintana-Fuentes, 2024). Likewise, time-frequency techniques such as the spectrogram, Hilbert–Huang Transform (HHT), and Wigner–Ville distribution suffer from limitations including fixed resolution, interference terms, and reduced performance in noisy environments (Flandrin, 1999; Scozzese and Dall'Asta, 2024). This methodological bottleneck underscores the need for new mathematical tools capable of analyzing seismic and oceanic signals with both high resolution and adaptivity across multiple scales.

ISSN-e 2395-8251

To address these limitations, we introduce the application of the Te-gram, a novel mathematical tool derived from the Te Transform (Trutie et al., 2021; Seuret-Jimenez et al., 2023; Trutié-Carrero et al., 2023a; Trutié-Carrero et al., 2023b), which was recently proposed by Seuret-Jimenez et al. (2023). The Te-gram enables the computation of the energy density distribution of a signal in a dyadic scale-frequency domain, providing a spectrogram of exceptional resolution that isolates dominant frequencies and attenuates cross terms. Unlike classical techniques, this tool adapts to the local characteristics of the signal, allowing for the identification of spectral components that may be masked in traditional analyses. The Te-gram is especially effective for stochastic and non-stationary data, where classical assumptions fail, and conventional transforms blur spectral boundaries.

The present study applies the Te-gram to investigate potential energetic correspondences between coastal wave activity and microseismic signals recorded along the northwestern coast of Mexico, with a focus on the Baja California region. Through the application of the Te-gram, we identify consistent frequency peaks at 0.07 Hz in both wave and seismic signals —coinciding with the primary microseismic band— and at 0.14 Hz in the seismic records, corresponding to secondary microseisms. These spectral alignments are not interpreted as direct causal triggers of seismic events but rather as manifestations of energy transfer mechanisms between the hydrosphere and the lithosphere. Our analysis confirms the theoretical frameworks of Hasselmann (1963) and Longuet-Higgins (1950) and offers a refined method for examining their spectral consequences with greater precision.

Furthermore, we propose a conceptual model in which the coastal wave–seismic interaction system behaves analogously to an astable oscillator. While the model remains qualitative in its current form, its

conceptual value lies in framing the system as an open energy accumulator—a perspective aligned with the fragment-asperity interaction model proposed by Sotolongo-Costa and Posadas (2004), and compatible with stress accumulation theories under cyclic ocean loading (Wang and Koblinsky, 1994; Berger et al., 2004).

The remainder of the paper is structured as follows. The Theoretical Background section presents the theoretical framework of the study, including the formal definition of the Te-gram and the coastal-wave oscillator model. The Results section details the empirical methodology and presents the main findings of the spectral analysis. The Discussion section provides a critical interpretation of the findings and their implications for seismological theory. Finally, the Conclusions section summarizes the study's main conclusions and outlines future research directions that may leverage this approach in the context of seismic hazard assessment and geophysical monitoring.

THEORETICAL BACKGROUND

In this section, the authors present the methods and tools used to demonstrate the relationship between coastal wave shock and Earth noise based on microseismic spikes. The model that supports this study and the definition of the Te-gram are presented.

Coastal-Wave Model

To conceptualize the interaction between coastal ocean waves and tectonic stress release mechanisms, we propose a phenomenological framework inspired by nonlinear energy accumulation systems. Although traditional earthquake generation is modeled through stick-slip dynamics governed by elastic rebound theory, alternative formulations such as the fragment–asperity interaction model (Sotolongo-Costa and Posadas, 2004) allow for a broader interpretation of stress accumulation influenced by external forces.

Here, we adopt an analogical representation in which the ocean–lithosphere system behaves as a nonlinear astable oscillator (Millman and Taub, 1965), akin to a multivibrator circuit, wherein wave energy input acts as a dynamic capacitance and interplate friction represents a variable resistance. In this analogy, coastal wave energy continuously charges the system; when the energy surpasses the critical friction threshold between tectonic asperities, a rapid energy discharge occurs— manifesting as seismic rupture. While the analogy is qualitative, it aligns conceptually with observations of cyclical energy input and irregular release in seismically active subduction zones (Wang and Koblinsky, 1994; Berger et al., 2004).

This model highlights a potential modulation of tectonic stress regimes by oceanic forcing. Though we do not claim a deterministic trigger mechanism, our spectral analysis suggests that persistent frequency-energy correspondence between ocean wave impacts and background seismic noise could reflect a long-term coupling process that merits further quantitative modeling and validation.

Te-gram

The Te-gram is a mathematical tool designed to analyze the energy density distribution of signals in the scale-frequency domain. It is derived from the Te Transform—a high-resolution integral transform introduced by Trutie et al. (2021)—and is particularly suitable for the analysis of non-stationary and stochastic signals, such as ambient seismic noise and ocean wave time series.

Formally, the Te-gram of a signal $f(t)$ is defined as:

ISSN-e 2395-8251

$$\Lambda[f(t)](\mu,\xi,\vartheta) = \left|\langle f, g_{\mu,\xi,\vartheta}\rangle\right|^2 = \left|\int_{-\infty}^{\infty} f(t) g^*_{\mu,\xi,\vartheta}(t)dt\right|^2, \quad (1)$$

where

$\Lambda[f(t)](\mu,\xi,\vartheta)$ denotes the Te-gram, and

$\left|\langle f, g_{\mu,\xi,\vartheta}\rangle\right|^2$ represents the energy density of $f(t)$ in the Te domain.

$g_{\mu,\xi,\vartheta}(t) = \omega_\mu(t)\psi_{\xi,\mu}(t)e^{i2\pi\vartheta t}$ is a localized wavelet-like kernel in $L^1(\mathbb{R}) \bigcap L^2(\mathbb{R})$, constructed using a Daubechies 45 mother function and a Kaiser-6 window function, providing strong frequency selectivity and cross-term suppression.

$\psi_{\xi,\mu}(t) = \frac{1}{\sqrt{2^\xi}}\psi\left(\frac{t}{2^\xi} - \mu\right)$ is the scaled and translated Daubechies 45 mother function, and

$\omega_\mu(t) = \omega(t-\mu)$ is the translated Kaiser-6 window function.

The parameter ϑ denotes the dyadic linear frequency, whereas ξ and μ correspond to the scale and translation parameters of the wavelet, respectively (Seuret-Jimenez et al., 2023).

The main advantages of the Te-gram over classical methods such as the Short-Time Fourier Transform (STFT), Hilbert–Huang Transform (HHT), or Wigner–Ville distribution include:

- Dyadic frequency decomposition, which enables the identification of frequency bands with maximal energy density.
- Superior spectral resolution, particularly in closely spaced frequency components.
- Reduced interference terms, ensuring clearer identification of dominant modes in noisy environments.
- Multiscale sensitivity, adaptable to both deterministic and stochastic signal structures.

These properties make the Te-gram especially powerful in the context of microseismic analysis, where overlapping frequency components, long-duration low-frequency oscillations, and non-Gaussian signal behavior often hinder interpretation with conventional techniques.

Data sources used

This study utilizes two synchronized datasets from geophysically significant locations in northwestern Mexico:

1. Seismic Data: Obtained from the Tijuana broadband seismic station (TJIG) of the Mexican National Seismological Service (SSN), located at 32.433°N, 116.676°W. We use the vertical component (HLZ) of ground-acceleration time series (accelerograms), sampled at 1 Hz, covering a one-hour window around each selected seismic event.
2. Ocean Wave Data: Acquired from the Coastal Data Information Program (CDIP), specifically from Station 155 (Imperial Beach Nearshore, California), located at 32.569°N, 117.135°W. The buoy records directional wave spectra and displacement time series, including vertical buoy displacements. Vertical buoy acceleration is estimated by taking the second time derivative of the displacement signal and is then normalized against the seismic data for spectral comparison.

ISSN-e 2395-8251

To mitigate noise introduced by numerical differentiation, especially in high-frequency components, we apply the Savitzky–Golay filter before derivative computation. This filter is chosen for its ability to preserve signal peaks and temporal structure while minimizing distortion in localized features (Guevara, 2019).

The computational implementation and signal processing are performed in MATLAB. All-time series are processed at a common sampling frequency of 1 Hz to comply with the Nyquist sampling criterion and are time-aligned to ensure comparability (Essen et al., 1999). For the seismic signals, the mean value is removed to eliminate the DC offset, and the resulting signals are normalized by their maximum absolute amplitude before applying the Te-gram. For each seismic event, two analysis scenarios are considered: a 1-hour interval on the day of the earthquake, including the mainshock, and an equivalent 1-hour interval two days before the earthquake, used as a control for identifying persistent energy structures. Figure 1 summarizes the computational workflow applied to both seismic and ocean wave signals.

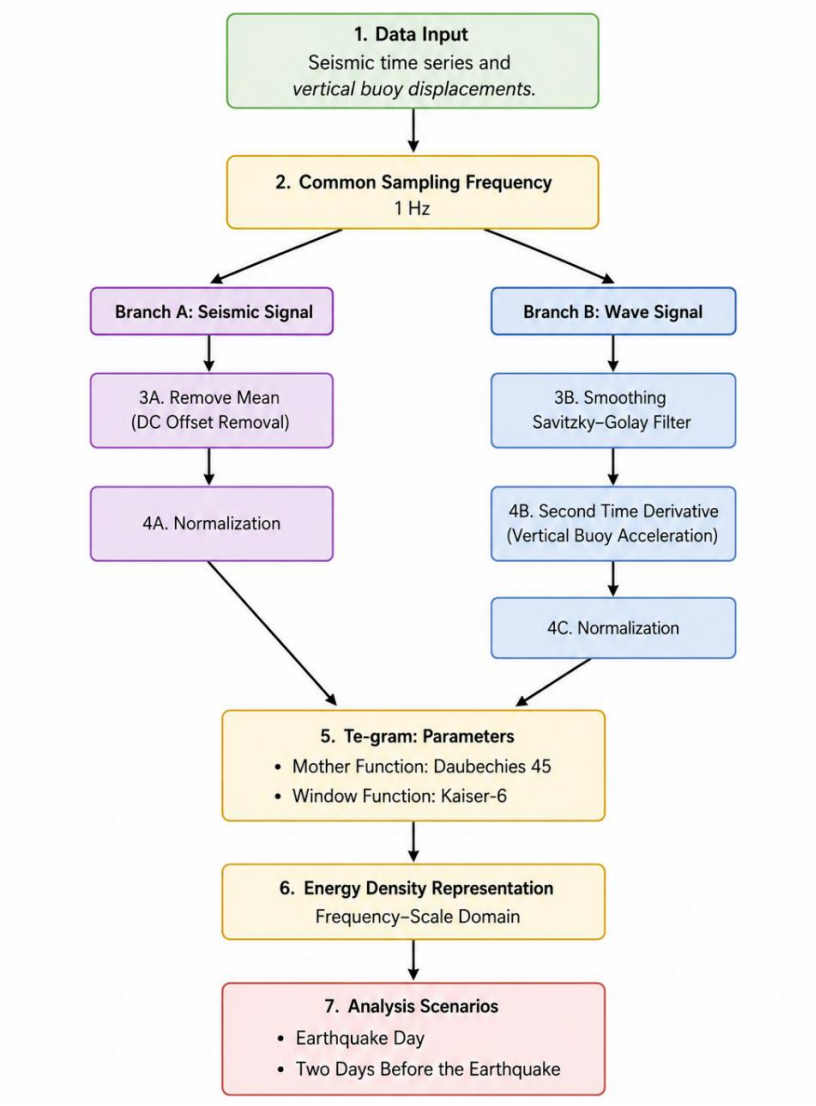

Figure 1. Computational workflow for applying the Te-gram to seismic and ocean wave signals. Source: Author's work.

ISSN-e 2395-8251

RESULTS

In this section, the authors present the results obtained by applying Te-gram to time-series signals of wave and seismic activity. As a result, it was possible to demonstrate the hypothesis proposed in this paper regarding the relationship between wave pounding on the coast and Earth's noise in the northwest of Mexico.

The analysis focused on two distinct seismic events recorded along the coast of Baja California, Mexico, for which high-quality oceanographic and seismic data were simultaneously available. Both events present an optimal spatial configuration for high-resolution spectral analysis due to the proximity of two instrumental platforms: the Tijuana Broadband Seismic Station (TJIG) and the Imperial Beach Coastal Buoy (CDIP Station 155) (see Figure 2). This spatial arrangement provides a quasi-synchronous record of ocean wave dynamics and seismic ground motion originating from the same coastal boundary layer, improving comparative spectral analysis. The first event occurred on April 22, 2021, and the second on February 3, 2022. For each event, two different scenarios were analyzed: the wave and seismic signals recorded on the day of the earthquake and the corresponding signals recorded two days before the event. Equivalent time intervals were considered in both scenarios to provide a consistent basis for comparison. The results obtained are presented in the following sections.

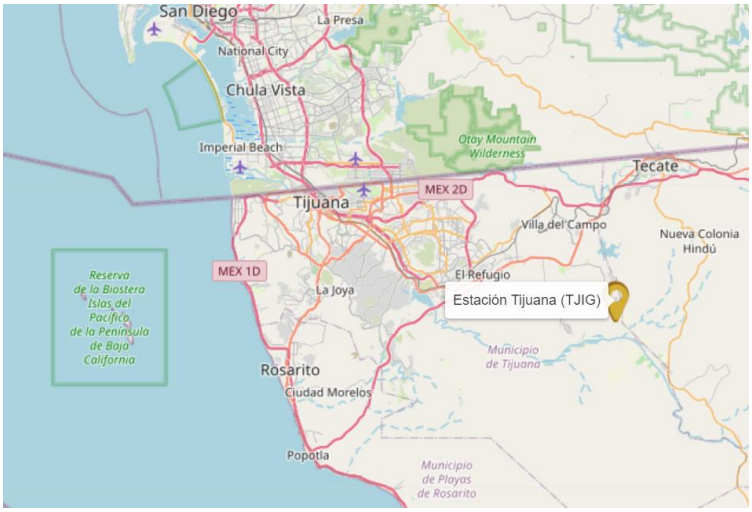

Figure 2. Map of the southwest of "Playas de Rosarito", state of Baja California, Mexico. Source: (México SSN Servicio Sismológico Nacional, 2024).

Earthquake of April 22, 2021

The earthquake on April 22, 2021, at 06:47:21 UTC, with a magnitude of 3.8, had its epicenter 39 km southwest of "Playas de Rosarito" in the state of Baja California, at a latitude of 32.351° N and a longitude of -117.302° W (México SSN Servicio Sismológico Nacional, 2024). Its proximity to the Tijuana seismological station and the directional buoy at Imperial Beach allowed the authors of this manuscript to obtain the necessary information for the proposed analysis.

ISSN-e 2395-8251

Analysis of wave and seismic signals on April 22, 2021

- Analysis of wave signals

Figure 3 displays the time-domain representation of the vertical buoy acceleration during the selected interval. The signal exhibits modulation in amplitude and envelope structure, indicative of incoming long-period wave groups.

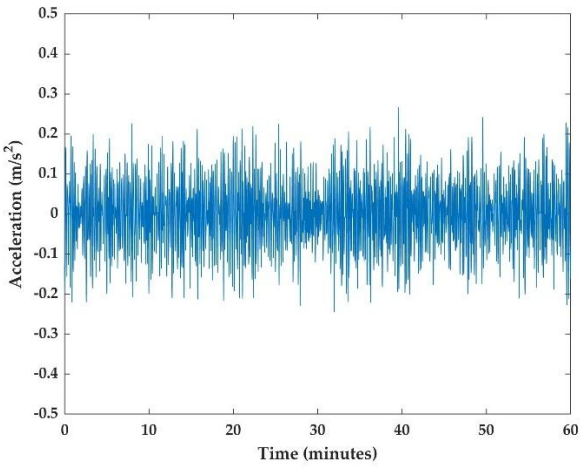

Figure 3. Time-domain representation of the vertical buoy acceleration from 06:00:00 to 07:00:00 UTC on the day of the earthquake, April 22, 2021. Source: Author's work.

ISSN-e 2395-8251

Since the time domain does not clearly reflect the spectral characteristics of the signal, spectral analysis is necessary. Analyzing signals in the frequency domain using appropriate signal processing tools allows their spectral components to be identified and characterized. Some of the signal processing tools that offer this advantage are: the Spectrogram of a signal (Quintana-Fuentes, 2024), the Hilbert–Huang Transform (Scozzese and Dall'Asta, 2024), the Wigner–Ville distribution (Sharma, 2024), and the Gabor Transform (Liu et al., 2024).

Figure 4 illustrates the spectral results obtained by applying these methods to the vertical buoy acceleration signal shown in Figure 3. Each method was implemented following standard parameterizations from the literature to ensure a fair comparison.

Figure 4(a) shows the spectrogram generated by STFT, which uses a fixed Gaussian window. While it reveals a general energy band between 0.05 Hz and 0.1 Hz, the spectral resolution is insufficient to isolate a dominant frequency component. The smoothing caused by the fixed window size blurs the time-frequency representation, making it difficult to attribute energy peaks to specific wave frequencies.

Figure 4(b) presents the result of the Hilbert–Huang Transform, which decomposes the signal into Intrinsic Mode Functions (IMFs) and computes the Hilbert spectrum. Although this method is adaptive and nonlinear, the resulting spectrum exhibits significant mode mixing and amplitude leakage. The 0.07 Hz component appears weak and poorly resolved, reflecting the method's sensitivity to noise and signal irregularities.

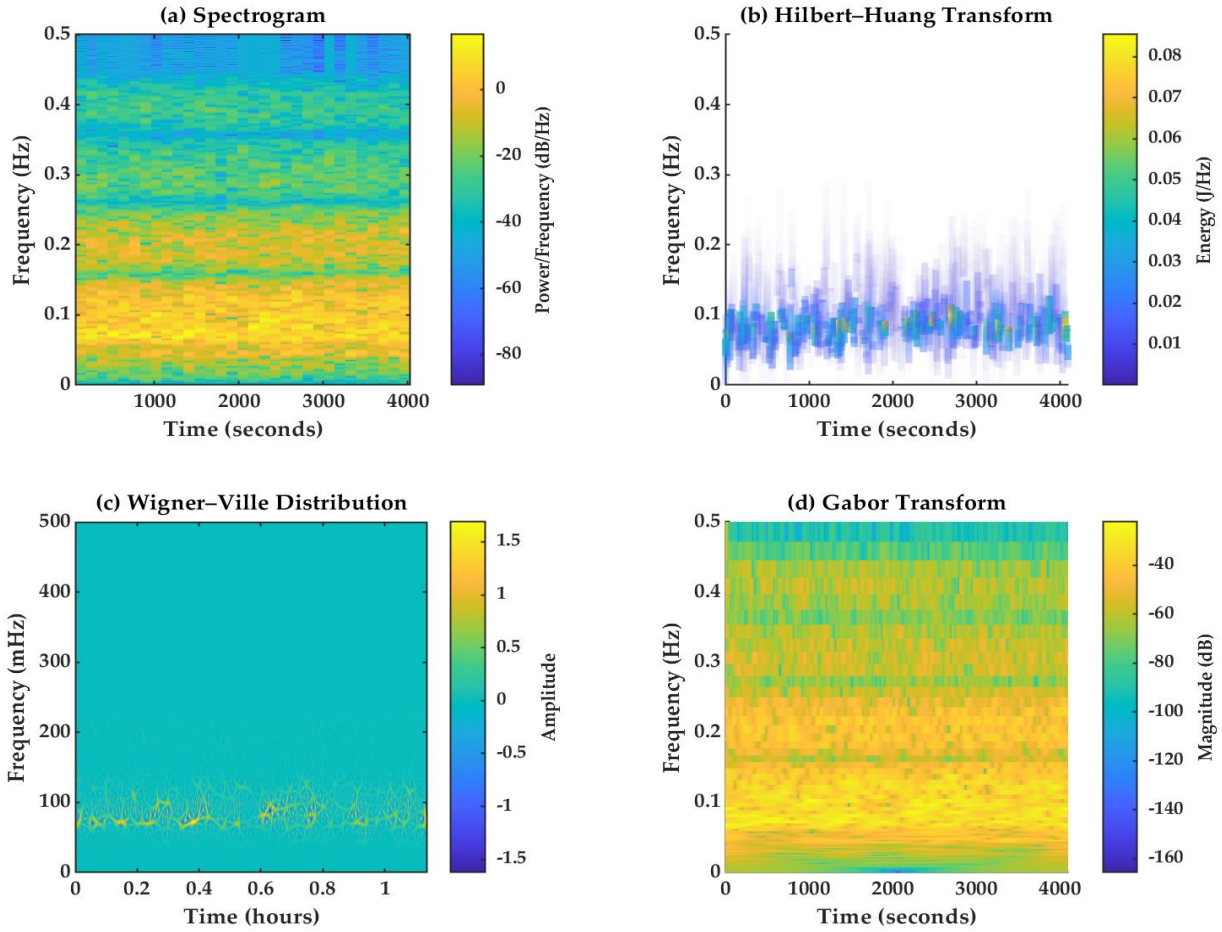

Figure 4. Results obtained by applying the methods reported in the reviewed literature to the vertical buoy acceleration signal. Source: Author's work.

Figure 4(c) displays the Wigner–Ville distribution. This bilinear method offers high theoretical resolution but suffers from strong cross-term interference. The resulting time-frequency map is cluttered with non-physical artifacts, masking the true spectral content of the signal. The dominant frequency cannot be reliably extracted due to these interference patterns.

Figure 4(d) shows the Gabor Transform output, which applies a Gaussian-modulated sinusoidal kernel to the signal. Although Gabor analysis offers a compromise between time and frequency localization, it also fails to extract a sharply defined spectral peak. The representation reveals a diffused energy band between 0.06 Hz and 0.1 Hz, but with insufficient contrast or focus at 0.07 Hz.

It is important to note that the methods reported in scientific literature are mainly based on time-frequency analysis. Therefore, Figure 5 presents the results of applying the Te-gram—the mathematical tool defined in this manuscript (see Figure 5a–b)—to the signal shown in Figure 3. This new application of the Te-gram employs the dyadic frequency spectrum approach to illustrate the energy distribution of a signal's frequency content in a frequency-scale plane ($\vartheta - \xi$), where ϑ denotes the dyadic linear frequency and ξ represents the scale parameter.

ISSN-e 2395-8251

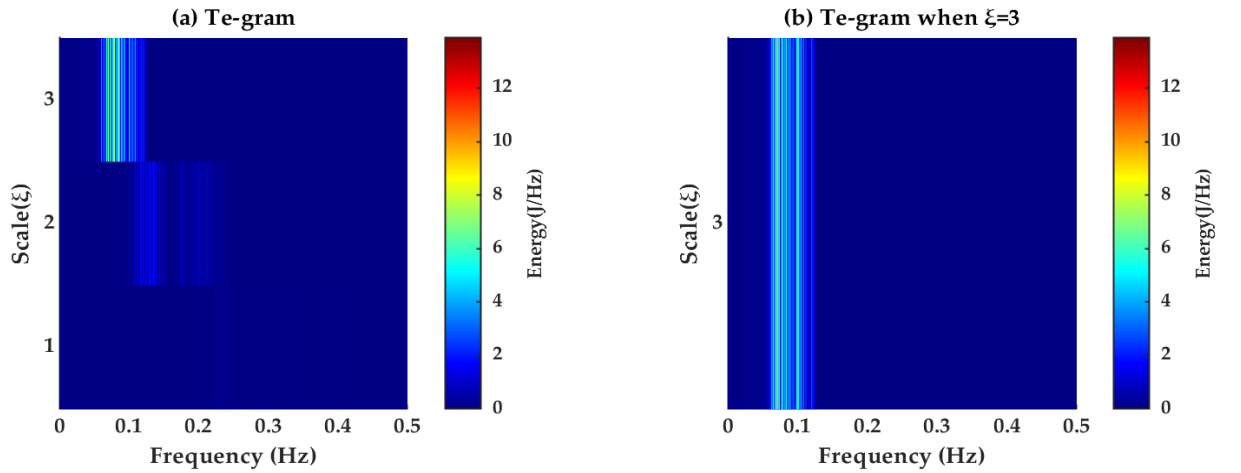

Figure 5. Results obtained from the application of Te-gram. (a) Te-gram of the vertical buoy acceleration signal on the day of the earthquake, April 22, 2021; (b) Te-gram when $\boldsymbol{\xi = 3}$. Source: Author's work.

It is important to highlight that the methods reported in the scientific literature are primarily based on time-frequency analysis. Figure 5 shows the spectral decomposition of the same acceleration signal using Te-gram. This method is based on the progressive fragmentation of the frequency spectrum into dyadic intervals, i.e., frequency intervals whose widths are successively reduced by factors of two. At each scale, the frequency range under analysis is divided into increasingly narrow sub-bands, allowing the spectral content to be examined with progressively higher frequency resolution. Instead of representing the signal using a single frequency partition with fixed resolution, the Te-gram offers a hierarchical representation in which spectral regions of interest can be successively refined. This property enables the analysis to focus on intervals where significant energy concentrations are detected, while simultaneously preserving information regarding their location within the original spectral structure (Seuret-Jimenez et al., 2023).

Panel (a) shows the dyadic scale-frequency map, while panel (b) presents the corresponding energy distribution as a function of frequency. Unlike the blurred or distorted outputs of classical methods, Te-gram isolates a well-defined spectral peak, centered at 0.07 Hz, with a localized energy density of 13.87 J/Hz. This frequency band (0.06–0.12 Hz) corresponds to the range of primary microseisms, typically associated with long-period wave activity interacting with the seafloor.

This characteristic, centered on the primary microseism band, aligns with the expected response of long-period waves interacting with the seafloor. The multiscale sensitivity and noise resistance of Te-gram allow these features to be resolved more accurately than conventional methods. The clear appearance of this spectral peak provides direct evidence of coherent coupling between waves and the seafloor during the event window.

- Analysis of seismic signals

To assess the lithospheric response during the April 22, 2021, earthquake, we analyzed the vertical ground acceleration recorded at the TJIG broadband station (approximately 60 km from the epicenter). The time window (06:00–07:00 UTC) was selected to match the analyzed ocean wave data, allowing for direct comparison. This timing reduces the likelihood that spectral similarities are due to background variability, strengthening the analysis of potential energy coupling at the ocean-solid earth interface.

ISSN-e 2395-8251

Preprocessing steps included instrumental response removal, baseline correction, and band-pass filtering between 0.01 Hz and 1 Hz to isolate the microseismic band. The signal was subsequently resampled to 1 Hz to match the temporal resolution of the buoy data and facilitate spectral comparison. A third-order Savitzky-Golay filter was also applied to suppress high-frequency noise while preserving low-frequency components critical for microseismic analysis.

Figure 6 shows the seismic acceleration signal. The waveform exhibits small-amplitude fluctuations before and after the mainshock, consistent with background microseismic activity. These fluctuations are especially relevant for understanding continuous ambient energy fields, as they can encode information about persistent coupling with external forcings, such as ocean wave activity.

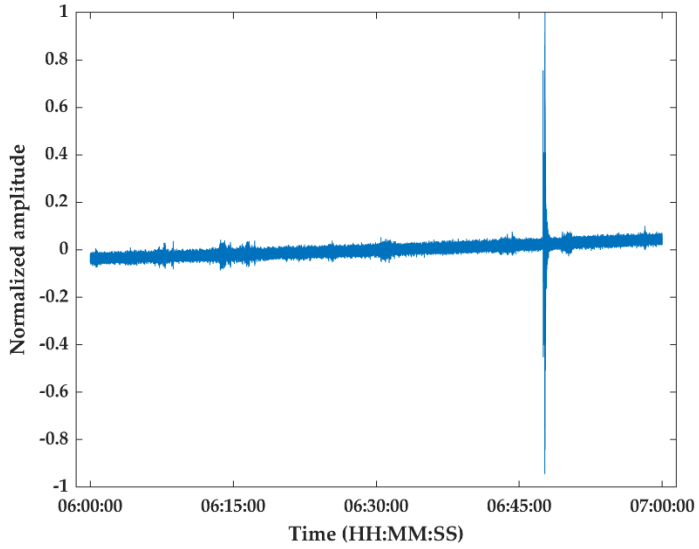

Figure 6. Representation of the normalized seismic signal in the time domain for the day of the earthquake, April 22, 2021, from 06:00:00 to 07:00:00 UTC. Source: Author's work.

The results obtained from the application of the Te-gram to the seismic signal are presented in Figure 7 (see Figure 7a-c). Figure 7(a) shows that in the analyzed signal, energy is concentrated in two particular frequency bands: one with lower energy ranging from 0.06 Hz to 0.12 Hz (see Figure 7b) with a higher predominance at a frequency of 0.07 Hz with 16,755 J/Hz, and a second frequency band ranging from 0.12 Hz to 0.24 Hz (see Figure 7c) with the highest energy concentration at the frequency of 0.14 Hz with 29,816 J/Hz. This alignment with the dominant wave frequency at the CDIP buoy strongly suggests the presence of an ocean-generated microseismic component superimposed on the tectonic signal.

ISSN-e 2395-8251

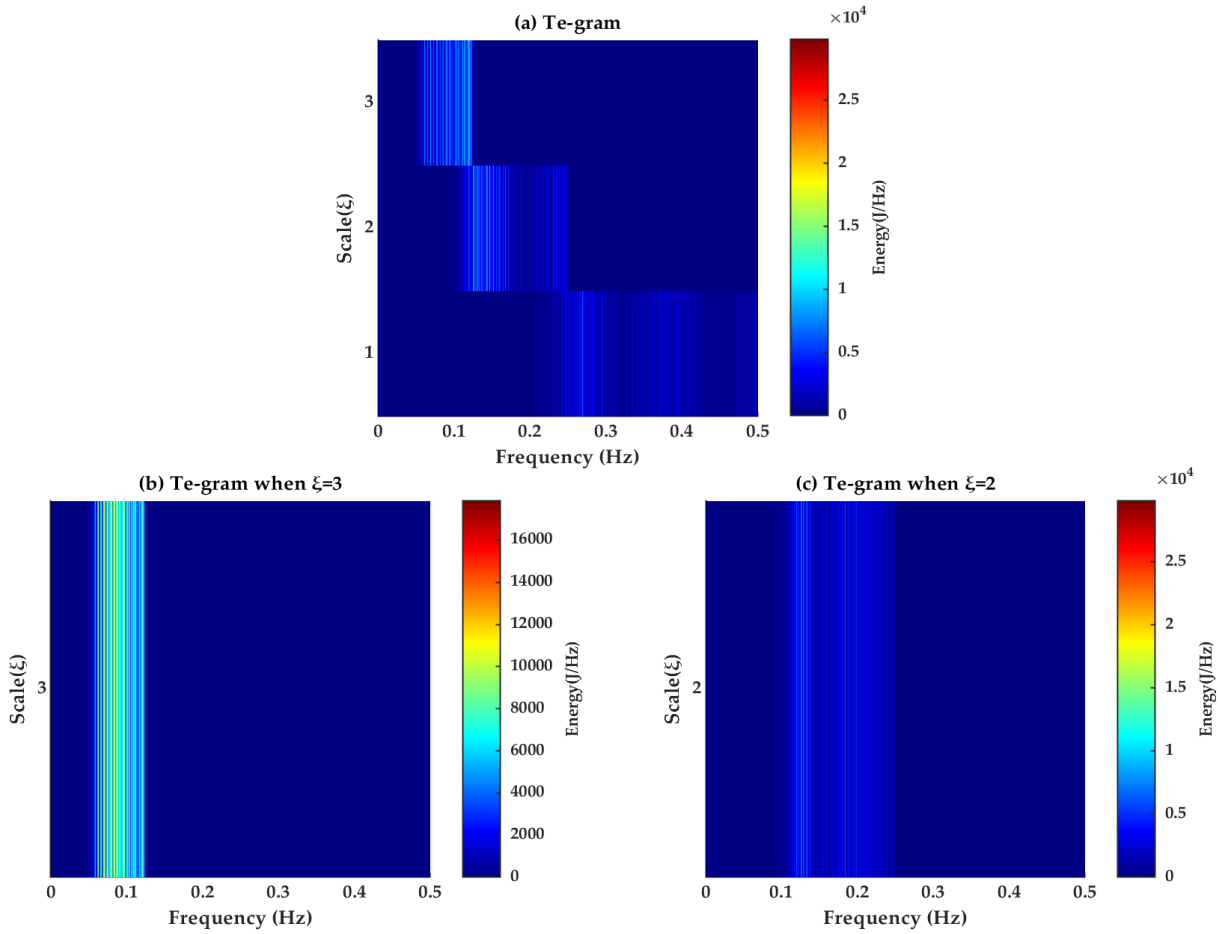

Figure 7. Results obtained from the application of the Te-gram. (a) Te-gram of the seismic signal from April 22, 2021; (b) Te-gram when $\xi = 3$; (c) Te-gram when $\xi = 2$. Source: Author's work.

Analysis of wave and seismic signals on April 20, 2021

The objective of this subsection is to present the results of applying the Te-gram to the wave and seismic noise signals two days before the earthquake occurred.

- Analysis of wave signals

Figure 8 shows the vertical buoy acceleration signal, estimated from the vertical displacement data obtained from the Imperial Beach buoy, in the time domain two days before the earthquake, using the same time interval as that considered on the day of the earthquake (06:00:00–07:00:00 UTC).

ISSN-e 2395-8251

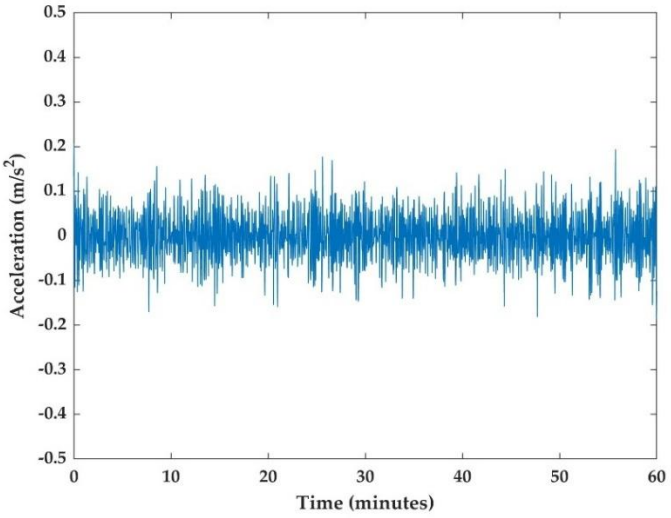

Figure 8. Representation of the vertical buoy acceleration signal in the time domain on April 20, 2021, from 06:00:00 to 07:00:00 UTC. Source: Author's work.

Figure 9 shows the application of the Te-gram to the signal of Figure 8. (see Figure 9a-b).

ISSN-e 2395-8251

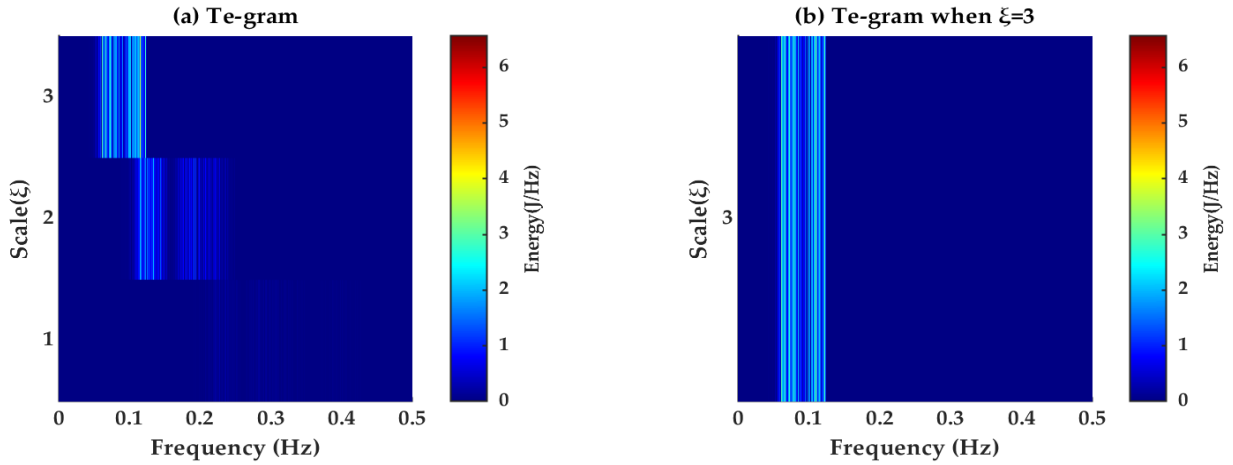

Figure 9. Results obtained from the application of the Te-gram to the vertical buoy acceleration signal two days before the earthquake, April 20, 2021. (a) Te-gram of the signal in Figure 8. (b) Te-gram when $\xi = 3$. Source: Author's work.

The results shown in Figure 9 reveal that two days before the earthquake, the wave spectrum exhibited a higher concentration of energy at scale 3 (see Figure 9a), corresponding to a frequency band in the range of 0.06 Hz to 0.12 Hz, with maximum energy of 6.56 J/Hz at the frequency component of 0.07 Hz (see Figure 9b).

- Analysis of seismic signals

An analysis of the application of the Te-gram to the seismic signal of April 20, 2021, as shown in Figure 10, is also conducted, with the results displayed in Figure 11.

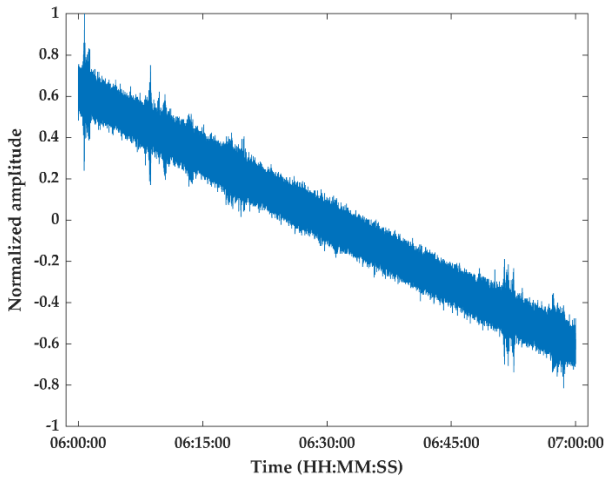

Figure 10. Time-domain representation of the seismic signal on April 20, 2021, from 06:00:00 to 07:00:00 hours UTC. Source: Author's work.

Applying this mathematical tool to the signal in Figure 10 reveals an energy concentration at scales 2 and 3 of the frequency spectrum shown in Figure 11(a). The energy concentrated at scale 3 corresponds to frequency components from 0.06 Hz to 0.12 Hz, with a peak energy of 15,978 J/Hz at the 0.07 Hz component (see Figure 11b). However, the maximum spectral energy values are at scale 2, covering a frequency range of 0.12 Hz to 0.25 Hz, with a peak at 0.14 Hz and an energy of 26,319 J/Hz (see Figure 11c).

The coincident spectral peaks at 0.07 Hz, observed in two independent data sets and recorded at distinct physical interfaces, support the hypothesis of wave-driven microseismic excitation. This comparative perspective reinforces the idea of a direct and measurable coupling mechanism between marine surface energy and terrestrial seismic responses.

This finding has important implications for passive seismology and marine geophysics, particularly in coastal regions, where microseismic energy can encode information about offshore wave conditions and interaction processes with the seafloor. Furthermore, Te-gram's success in resolving these features suggests its applicability as a robust tool for monitoring ocean-solid Earth coupling mechanisms, potentially enabling real-time environmental diagnostics using background seismic noise.

Earthquake of February 3, 2022

A second local earthquake was selected for spectral comparison to reinforce the generality of the observed ocean-lithosphere coupling mechanisms. This subsection presents the results obtained by applying Te-gram to the seismic and wave signals corresponding to the earthquake that occurred on February 3, 2022, at 09:55:32 UTC. This earthquake, with a magnitude of 3.9, had its epicenter 46 km southwest of Playas de Rosarito, Baja California, at a latitude of 31.941° N and a longitude of -117.19° W (México SSN Servicio Sismológico Nacional, 2024).

ISSN-e 2395-8251

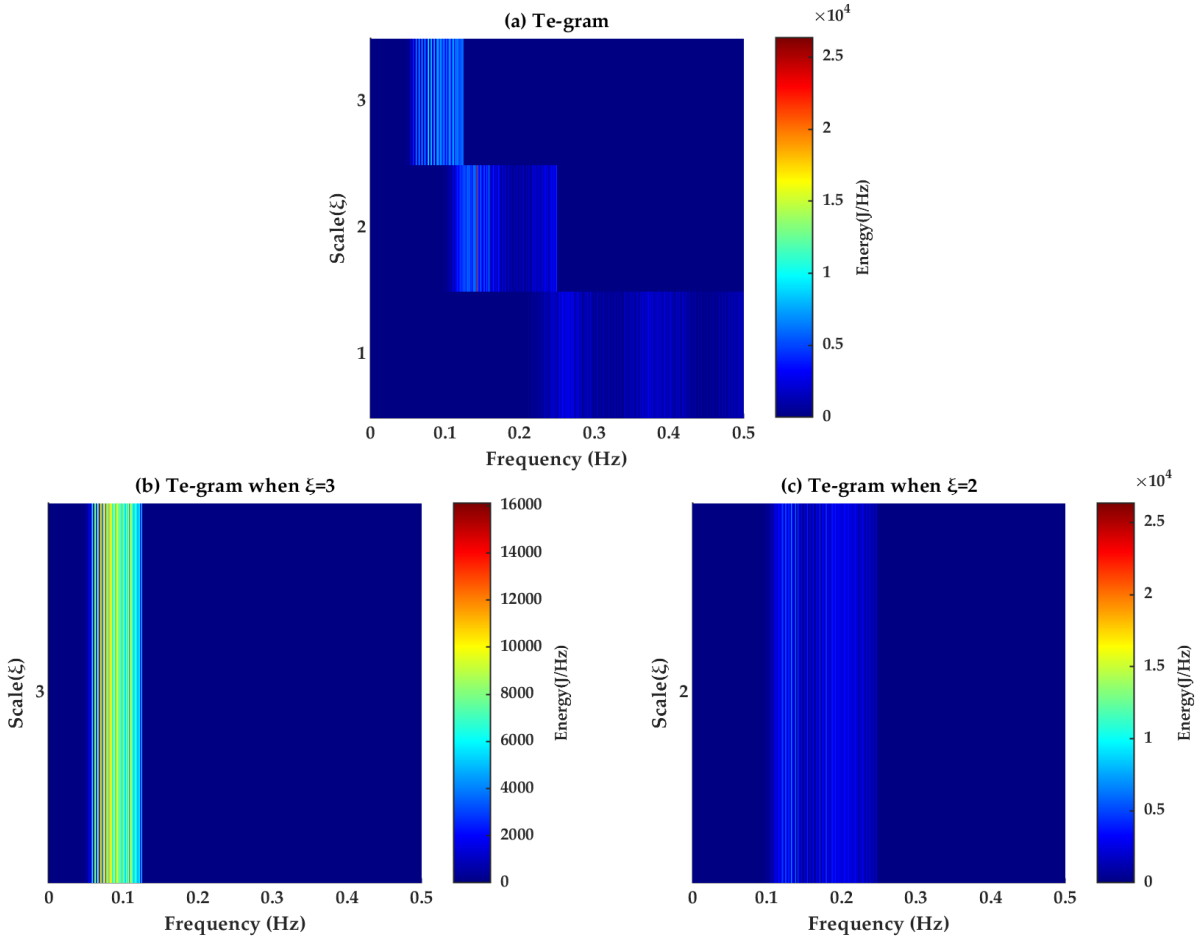

Figure 11. Application of the Te-gram two days before the earthquake, April 20, 2021. (a) Application of the Te-gram to the signal of Figure 10. (b) Te-gram when $\xi = 3$. (c) Te-gram when $\xi = 2$. Source: Author's work.

As described at the beginning of the Results section, the Te-gram analysis considered two scenarios for this event: the seismic and wave signals recorded on the day of the earthquake (February 3, 2022) and the corresponding signals recorded two days before the event (February 1, 2022). The results obtained are shown in Table 1.

Table 1 shows that the spectrum of ocean waves, both on the day of the earthquake and two days before, concentrates its energy at scale 3, specifically in the frequency component corresponding to 0.07 Hz. The magnitude of the energy varies, showing an increase from one day to the next: 6.96 J/Hz for February 1, 2022, and 9.33 J/Hz for the day of the earthquake.

Regarding the seismic signals, Table 1 displays information on the scales where the greatest concentration of energy is perceived: scale 3, which contains a notable presence of the frequency component of 0.07 Hz, and scale 2, with higher energy where the frequency component of 0.14 Hz is evident. The application of the Te-gram to seismic signals shows an increase in energy from February 1, 2022, to the day of the earthquake in both frequency components.

ISSN-e 2395-8251

Table 1. Results obtained with the application of the Te-gram to the seismic and wave signals on the day of the earthquake (February 3, 2022) and two days before (February 1, 2022). Source: Author's work.

Date of Analysis	Te-gram waves	Te-gram earthquakes	
	Scale 3	Scale 3	Scale 2
	Frequency - Energy	Frequency - Energy	Frequency - Energy
February 1, 2022	0.07 Hz - 6.96 J/Hz	0.07 Hz – 11 122 J/Hz	0.14 Hz – 11 261 J/Hz
February 3, 2022	0.07 Hz - 9.33 J/Hz	0.07 Hz – 20 877 J/Hz	0.14 Hz – 25 287 J/Hz

The findings from this second event support the robustness of the spectral methodology and suggest that the mechanisms underlying primary microseism generation are reproducible across events of moderate magnitude when oceanic forcing is stable, and instrumentation is optimally located. These results, when considered alongside the April 2021 analysis, provide convergent evidence for the role of ocean wave energy in modulating ambient seismic noise.

DISCUSSION

ISSN-e 2395-8251

The analysis of background seismic noise in relation to coastal ocean wave dynamics, presented in this study, offers compelling evidence of the energy transfer mechanisms that connect marine and solid-earth systems. The consistent spectral alignment at 0.07 Hz in both wave and seismic signals across two independent seismic events strengthens the hypothesis that long-period wave activity can influence microseismic energy levels. These findings open a new perspective on the excitation of primary microseisms, viewing them not only as stochastic background features but also as structured, frequency-specific responses to ongoing oceanographic forcing.

Conventional time-frequency methods (STFT, HHT, WVD, and Gabor) failed to resolve this dominant spectral peak, particularly in the presence of low signal-to-noise ratios and non-stationary dynamics. In contrast, the application of Te-gram provided improved localization, cross-term suppression, and adaptive resolution, which proved crucial for the identification of fine-scale spectral signatures. The successful discrimination of the 0.07 Hz component in seismic and waveform records, during distinct events and with different signal morphologies, highlights the robustness and transferability of the method for the analysis of multiscale geophysical signals.

From a physical standpoint, the detection of consistent energy peaks within the microseismic band supports previous studies proposing that infragravity wave components (below 0.1 Hz) may generate primary microseisms through direct interaction with the seafloor in shallow coastal environments (Hasselmann, 1963; Ardhuin et al., 2011). The spectral consistency across control periods and event windows suggests that such interactions may not only occur during extreme ocean conditions (e.g., storms) but may also be sustained under moderate, persistent swell regimes. This aligns with recent advances in marine seismology that emphasize the importance of continuous, low-amplitude coupling over episodic excitation (Stutzmann et al., 2012; Retailleau et al., 2018).

Additionally, the temporal coincidence of enhanced microseismic energy and local seismic activity, as observed in the April 22, 2021, event, raises provocative questions about the potential role of marine wave energy in modulating stress regimes near tectonic boundaries. While causality cannot be established

in this framework, the spatiotemporal alignment warrants further investigation using coupled mechanical and hydrodynamic models. In particular, the possibility that persistent microseismic forcing could affect fault lubrication, pore pressure, or trigger low-frequency tremors deserve deeper exploration, especially in regions with active subduction zones or transform boundaries.

Moreover, the methodological innovation presented here offers a scalable framework for passive monitoring applications. The ability of the Te-gram to resolve fine-grained spectral features in both seismic and marine data opens the door to its use in environmental surveillance, coastal engineering, early warning systems, and the study of slow geodynamic processes. In regions lacking dense seismic networks, buoys or coastal stations equipped with high-resolution spectral analytics may offer valuable insight into subsurface dynamics.

Finally, the application of this framework to two different seismic events—separated by over a year—demonstrates the reproducibility of the technique and the generality of its findings. The relationship coherence of the results supports the hypothesis that the 0.07 Hz frequency band represents a persistent marker of ocean–solid Earth coupling. Future work should focus on extending this methodology to other geographical settings, evaluating seasonal and bathymetric influences, and integrating this approach with three-dimensional numerical simulations of wave-induced ground motion.

CONCLUSIONS

ISSN-e 2395-8251

This work provides rigorous spectral evidence of an interaction between ocean wave dynamics and background seismic noise in a near-coastal environment, with a focus on primary microseisms. Using the Te-gram, we successfully isolated persistent energy peaks around 0.07 Hz in both seismic and oceanographic signals, a feature that remained unattainable with classical time-frequency analysis techniques.

The two seismic events analyzed (April 22, 2021, and February 3, 2022) showed not only a coincidence with local ocean wave activity but also strong spectral congruence within the microseismic band. These findings support the hypothesis that long-period waves in coastal regions act as a sustained source of ground motion by directly modulating pressure at the ocean-seafloor interface. The observed alignment suggests a more systematic and reproducible continuous energy transfer mechanism than previously assumed.

Furthermore, the control period analysis reinforces the interpretation that the 0.07 Hz spectral signature is not an artifact of transient seismicity or atmospheric variability, but rather an inherent feature of ambient seismic noise influenced by marine conditions. The relative increase in localized energy during seismic events, compared to background levels, could indicate a modulating role of oceanic forcing on stress conditions along shallow fault systems.

The new approach used in this study is revealed as a key methodological advance, which exceeds the capabilities of conventional approaches. By precisely elucidating the relationship between the energy of the waves and microseisms, this work not only confirms fundamental theories in seismology and oceanography but also enhances our understanding of how natural phenomena interact at micro and macro scales.

Importantly, this study introduces a methodological framework that integrates oceanographic and seismic data through the application of an advanced spectral tool, opening new avenues for interdisciplinary monitoring of the ocean-solid Earth system. Future research should aim to combine this spectral approach with mechanistic models of wave-seafloor coupling, inversion techniques for source parameter estimation,

and long-term seismic records to assess whether persistent spectral signatures can serve as precursors or modulators of seismic activity in nearshore tectonic regimes.

ACKNOWLEDGMENTS

The authors thank the Research Center for Engineering and Applied Sciences, Universidad Autónoma del Estado de Morelos, SECIHTI Mexico, and the National Seismological Service (SSN) for their support and data provided for this research.

REFERENCES

Ardhuin, F., Gualtieri, L. and Stutzmann, E. (2015) 'How ocean waves rock the Earth: Two mechanisms explain microseisms with periods 3 to 300s', *Geophysical Research Letters*, 42(3), pp. 765–772. Available at: https://doi.org/10.1002/2014GL062782.

Ardhuin, F., Stutzmann, E., Schimmel, M. and Mangeney A. (2011) 'Ocean wave sources of seismic noise', *JOURNAL OF GEOPHYSICAL RESEARCH*, 116(9), p. 21. Available at: https://doi.org/10.1029/2011JC006952.

Asten, M. (1978) 'Geological control of the three-component spectra of Rayleigh-wave microseisms.', *Bulletin of the Seismological Society of America*, 68, pp. 1623–1636.

Berger, J., Davis, P. and Ekström, G. (2004) 'Ambient Earth noise: A survey of the Global Seismographic Network', *Journal of Geophysical Research: Solid Earth*, 109(11), pp. 1–10. Available at: https://doi.org/10.1029/2004JB003408.

Bonnefoy-Claudet, S., Cotton, F. and Bard, P.Y. (2006) 'The nature of noise wavefield and its applications for site effects studies. A literature review.', *Earth-Science Reviews*, 79(3–4), pp. 205–227. Available at: https://doi.org/10.1016/j.earscirev.2006.07.004.

Buffoni, C. (2016) *Determinación de la estructura cortical en el sector argentino de la Isla Grande de Tierra del Fuego*. Available at: http://sedici.unlp.edu.ar/handle/10915/67907.

Castrillo, B.G. (2013) *ANÁLISIS Y APLICACIONES DEL RUIDO SÍSMICO EN MÉXICO, GOLFO DE MÉXICO Y CARIBE : TOMOGRAFÍA DE ONDAS SUPERFICIALES RAYLEIGH Y LOVE*.

Essen, H.-H., Klussmann, J., Herber R. and Grevemeyer I. (1999) 'Does microseisms in Hamburg (Germany) reflect the wave climate in the North Atlantic?', *Deutsche Hydrographische Zeitschrift*, 51(1), pp. 33–45. Available at: https://doi.org/10.1007/bf02763955.

Essen, H.-H. Krüger, F., Dahm, T., and Grevemeyer I. (2003) 'On the generation of secondary microseisms observed in northern and central Europe.', *Journal of Geophysical Research*, 108(B10), pp. 1–15. Available at: https://doi.org/10.1029/2002jb002338.

Flandrin, P. (1999) *Time-Frequency/Time-Scale Analysis.* Academic Press.

Friedrich, A., Krüger, F. and Klinge, K. (1998) 'Ocean-generated microseismic noise located with the Gräfenberg array', *Journal of Seismology*, 2(1), pp. 47–64. Available at: https://doi.org/10.1023/A:1009788904007.

Guevara, D.F. (2019) 'Preprocesamiento de los Datos de las Unidades de Medición Sincrofasorial (PMUs) utilizando la técnica limpieza de datos-Aplicación al Sistema Nacional Interconectado Ecuatoriano'. Available at: http://bibdigital.epn.edu.ec/handle/15000/19927.

ISSN-e 2395-8251

Haubrich, R. A., Munk, W. H., and Snodgrass, F. E. (1963) 'Comparative spectra of microseisms and swell', *Bulletin of the Seismological Society of America*, pp. 237–241. Available at: https://doi.org/10.1785/BSSA0530010027.

Hasselmann, K. (1963) *A statistical analysis of the generation of microseisms.*, *Institute of Geophysicsa nd Planetary Physics University o[California, San Diego*. Institute of Geophysicsa nd Planetary Physics University o[California, San Diego. Available at: https://doi.org/10.1029/RG001i002p00177.

Hinde, B.J. and Gaunt, D.I. (1967) 'Microseisms', *Contemporary Physics*, 8(3), pp. 267–283. Available at: https://doi.org/10.1080/00107516708204387.

Kedar, S., Longuet-Higgins, M., Webb, F., Graham, N., Clayton, R. and Jones, C. (2008) 'The origin of deep ocean microseisms in the North Atlantic Ocean', *Proceedings of the Royal Society A: Mathematical, Physical and Engineering Sciences*, 464(2091), pp. 777–793. Available at: https://doi.org/10.1098/rspa.2007.0277.

Liu, X., Li, S., Liu, H., He, L., and Liu, T. (2024) 'Infrared spectrum resolution enhancement model via Gabor transform regularization for object detection', *Infrared Physics & Technology*, 141. Available at: https://doi.org/10.1016/j.infrared.2024.105441.

Longuet-Higgins, M.S. (1950) *A theory of the origin of microseisms*, *Department of Geodesy and Geophysics, University of Cambridge*. Available at: https://doi.org/10.2307/j.ctt211qv60.7.

Lunansky, M. (2019) *Análisis del ruido sísmico mediante interferometría para el modelado cortical en la cuenca Chaco-Paraná*. Universidad Nacional de La Plata, Argentina.

México SSN Servicio Sismológico Nacional (2024). Available at: http://www.ssn.unam.mx/.

Millman, Jacob; Taub, H. (1965) 'Capitulo 11 - Multivibradores Monoestables y Astables', in *Pulse, Digital and Switching Waveforms*.

Nishida, K., Kawakatsu, H., Fukao, Y. and Obara, K. (2008) 'Background Love and Rayleigh waves simultaneously generated at the Pacific Ocean floors', *Geophysical Research Letters*, 35(16), pp. 1–5. Available at: https://doi.org/10.1029/2008GL034753.

Quintana-Fuentes, D. (2024) *Aplicación del te-gram al análisis del espectro de fugas de agua*. Universidad Autónoma del Estado de Morelos.

Retailleau, L. and Gualtieri, L. (2021) 'Multi-phase seismic source imprint of tropical cyclones', *Nature Communications*, 12(1), pp. 1–8. Available at: https://doi.org/10.1038/s41467-021-22231-y.

Retailleau, L., Landès, M., Gualtieri, L., Shapiro, N.M., Campillo, M., Roux, P., and Guilbert, J. (2018) 'Detection and analysis of a transient energy burst with beamforming of multiple teleseismic phases', *Geophysical Journal International*, 212(1), pp. 14–24. Available at: https://doi.org/10.1093/gji/ggx410.

Schulte-Pelkum, V., Earle, P.S. and Vernon, F.L. (2004) 'Strong directivity of ocean-generated seismic noise.', *Geochemistry, Geophysics, Geosystems*, 5(3), pp. 1–13. Available at: https://doi.org/10.1029/2003GC000520.

Schweitzer, J. (1911) 'Early German Contributions to Modern Seismology', *International Handbook of Earthquake and Engineering Seismology, edited by: Lee, W., Kanamori, H., Jennings, P., and Kisslinger, C., Elsevier*, pp. 1–57.

Scozzese, F. and Dall'Asta, A. (2024) 'Nonlinear Response Characterization of Post-Tensioned R . C . Bridges through Hilbert – Huang Transform Analysis', *Wiley* [Preprint]. Available at: https://doi.org/10.1155/2024/5960162.

ISSN-e 2395-8251

Seuret-Jiménez, D., Trutié-Carrero, E., Nieto-Jalil, J. M., García-Aquino, E. D., Díaz-González, L., Carballo-Sigler, L., Quintana-Fuentes, D., and Gaggero-Sager, L. M. (2023). Feature Extraction of a Non-Stationary Seismic–Acoustic Signal Using a High-Resolution Dyadic Spectrogram. Sensors, 23(13), 6051. https://doi.org/10.3390/s23136051 (2023) 'Feature Extraction of a Non-Stationary Seismic–Acoustic Signal Using a High-Resolution Dyadic Spectrogram', *Sensors*, 23(13). Available at: https://doi.org/10.3390/s23136051.

Sharma, A. (2024) 'Steel truss bridge damage assessment using kurtosis, FFT, spectrogram and Wigner-Ville distribution techniques'. Available at: https://doi.org/10.1504/IJQET.2024.142217.

Shubladze, T.A. and Tsereteli, N.S. (2023) 'Investigation of Ambient Seismic Noise in Different Region of Georgia', *Journals of Georgian Geophysical Society*, 26(2), pp. 5–12. Available at: https://doi.org/10.60131/ggs.2.2023.7428.

Sotolongo-Costa, O. and Posadas, A. (2004) 'Fragment-Asperity Interaction Model for Earthquakes', *Physical Review Letters*, 92(4), p. 4. Available at: https://doi.org/10.1103/PhysRevLett.92.048501.

Stehly, L., Campillo, M. and Shapiro, N.M. (2006) 'A study of the seismic noise from its long-range correlation properties', *Journal of Geophysical Research: Solid Earth*, 111(10), pp. 1–12. Available at: https://doi.org/10.1029/2005JB004237.

Stutzmann, E., Ardhuin, F., Schimmel, M., Mangeney, A. and Patau, G. (2012) 'Modelling long-term seismic noise in various environments.', *Geophysical Journal International*, 191(2), pp. 707–722. Available at: https://doi.org/10.1111/j.1365-246X.2012.05638.x.

Tanimoto, T. (2007) 'Excitation of microseisms', *Geophysical Research Letters*, 34(5), pp. 1–4. Available at: https://doi.org/10.1029/2006GL029046.

Tanimoto, T., Ishimaru, S. and Alvizuri, C. (2006) 'Seasonality in particle motion of microseisms', *Geophysical Journal International*, 166(1), pp. 253–266. Available at: https://doi.org/10.1111/j.1365-246X.2006.02931.x.

Traer, J. and Gerstoft, P. (2014) 'A unified theory of microseisms and hum', *Journal of Geophysical Research: Solid Earth*, 119(4), pp. 3317–3339. Available at: https://doi.org/10.1002/2013JB010504.

Trutie, E., Seuret-Jiménez, D. and Nieto-Jalil, J.M. (2021) 'A High-Resolution Dyadic Transform for Non-Stationary Signal Analysis', *Mathematics* [Preprint].

Trutié-Carrero, E., Seuret-Jiménez, D., Nieto-Jalil, J. M., Cantó, J., Valdés-Santiago, D., and Carballo-Sigler, L. (2023) 'The Te Transform: A High-Resolution Integral Transform and Its Key Properties', *Mathematics*, 11(21). Available at: https://doi.org/10.3390/math11214495.

Trutié-Carrero, E., Seuret-Jiménez, D., Nieto-Jalil, J. M., Herrera-Díaz, J. C., Cantó, J., and Escobedo-Alatorre, J. J. (2023) 'Detection of Background Water Leaks Using a High-Resolution Dyadic Transform', *Water (Switzerland)*, 15(4). Available at: https://doi.org/10.3390/w15040736.

Wang, C., and Koblinsky, C.J. (1994) 'Low-frequency response of sea level to atmospheric forcing in the North Pacific Ocean.', *Journal of Physical Oceanography*, 24, pp. 664–675. Available at: https://doi.org/10.1175/1520-0485(1994)024.

Webb, S.C. (2007) 'The Earth's "hum" is driven by ocean waves over the continental shelves', *Nature*, 445(7129), pp. 754–756. Available at: https://doi.org/10.1038/nature05536.

ISSN-e 2395-8251